Available online at www.sciencedirect.com
SCIENCE DIRECT®
Computers and Structures 81 (2003) 2549–2556
Computers & Structures
www.elsevier.com/locate/compstruc

Joint stiffness identification using FRF measurements

Tachung Yang [a,*], Shuo-Hao Fan [a], Chorng-Shyan Lin [b]

[a] Department of Mechanical Engineering, Yuan Ze University, 135 Far East Road, Neili, Taoyuan 32026, Taiwan
[b] Chung-Shan Institute of Science and Technology, Lung-Tan, Taoyuan, Taiwan

Received 16 July 2002; accepted 15 July 2003

Abstract

In this research, an identification method for joint parameters has been developed by using the substructure synthesis method and frequency response functions (FRFs). A matrix form for the joint model was proposed. Identifying the joint parameters of a beam screwed down at one of its end was conducted. Only two measurement points were used in the experiment. The simulated results of the FRFs of the constrained beam with the properly identified joint parameters agree with the experimental results very satisfactorily. The accuracy of the identified results is strongly sensitive to the parameters. The rotational stiffness of the screw joint is identified to be located in the sensitive region, so the identified result of the rotational stiffness is very good. However, the less accurate results for the translational stiffness located in the insensitive region do not affect apparently the accuracy of the simulated results. The cross-coupled term between the translational and rotational stiffness in the joint model was identified, which greatly improved the accuracy of the simulated FRFs in higher frequency regions.

Keywords: Joint identification; Substructure synthesis method; Stiffness; Rotational degree of freedom; Frequency response function

1. Introduction

A complicated structure is usually composed of substructures or subsystems. The substructure synthesis method is to integrate the results of analyses for the substructures and to predict the dynamic behavior of the assembled system. The substructures usually connect to each other by joints. This fact clearly indicates that the analyses will not properly model the dynamic behavior of the structure if the joints cannot be accurately identified [1,2]. Although the methods of model updating, using experimental results to modify an existing model, are applicable to the problems of joint identification. The nature of the two problems is different and special consideration is necessary on the modeling and flexibility of the joints [3]. How to build adequate models for joints and accurately identify parameters is the key point to the success of the dynamic analyses of structures.

Model parameters obtained from modal testing are widely used in the joint identification [4,5]. However, accurate modal parameters are not easily obtained for structures containing closely spaced modes or large modal damping [6]. The procedure of obtaining the modal parameters usually involves curve-fitting processes, which inevitably incorporate errors into the results. Direct use of frequency response function (FRF) can avoid this shortcoming; besides, the amount of data of frequency response is much more than that of modal parameters for joint identification from the same number of experiments.

Tsai and Chou [7] used the substructure synthesis method with FRFs to identify two types of bolted joints on overlapped beams. Wang and Liou [8] extended the work of Tsai and Chou [7]. They used diagonal matrices for joint modeling and an algorithm to reduce the noise

* Corresponding author. Tel.: +886-3-463-8800x456; fax: +886-3-455-8013.
E-mail address: mety@saturn.yzu.edu.tw (T. Yang).

0045-7949/$ - see front matter © 2003 Elsevier Ltd. All rights reserved.
doi:10.1016/S0045-7949(03)00328-6

effect. Hong and Lee [9] proposed a method using the measured FRFs of the structure and the computed FRFs of an auxiliary model. Hwang [10] numerically determined the spring constants of the joint by subtracting the inverted matrices of FRF of the structure with and without joints. An averaging process is used to reduce the noise effect, excluding the FRF near the resonance zones. However, these methods require or use the measured FRFs related to the joints, which are not easy to obtain in real structures.

Yang and Park [6] utilized frequency responses with the finite element model of the whole structure to identify the joint parameters by iteration. Three joint models are evaluated.

Ren and Beards [11] evaluated the substructure synthesis methods using FRFs from numerical viewpoints and physical viewpoints and proposed a generalized receptance coupling method for multiple connections.

Yang [12] studied the joint parameters in different situations and discussed the various techniques of substructure synthesis. He found that the identification results of damping are not good when the effects of stiffness and damping of the joint have large differences. Too large or too small deformation in the joint in the frequency range will result in poor identification accuracy. Techniques of weighting and sensitivity are used to reduce the identification errors.

Some research works considered only translational stiffness in the modeling of joints [8–10,12]. Due to the difficulty of measurement, the joint has been modeled as two parallel springs in regards to the effect of rotational stiffness [7]. This model works well in the low frequency range, but not very good in higher frequency range. Recently, more research results showed that the joint could be modeled by translational and rotational springs reasonably [6,13–15].

From the above literature, the major concerns about the implementation of the substructure synthesis method with measured FRFs can be summarized as: incompleteness of FRFs measurement, inaccessibility of the measurement at the joints, measurement noise [6], as well as adequacy of the joint model and parameter sensitivity [12]. This paper improved the methods of Tsai and Chou [7] and Wang and Liou [8], and derived the identification equations for joints. Special attention was given on the major concerns during the derivation. The method used the accurately calibrated finite element model of the unconstrained (or free–free) structure to obtain the necessary information of rotational degrees of freedom. Then, substructural synthesis method was used to identify the translational and rotational stiffness of the joint. The merit of this method is that only a limited number of the measured FRFs related to the translational degrees of freedom in the non-joint regions are needed. We considered the joint model as a coupled stiffness matrix, instead of a set of a translational spring and a rotational spring only. Damping arising in the joints was not addressed in this paper.

2. Theory

As shown in Fig. 1, the whole structure is composed of substructures 1 and 2, connected by the joints that are assumed to be formed by springs and dampers. Regions a and c represent the regions excluding the joints in substructures 1 and 2 respectively, and region b represents the region of joints. Assuming no external moment acting on the regions a and c, $\{m_a^{(1)}\} = 0$ and $\{m_c^{(2)}\} = 0$, the relationship between the input and the output of the substructure can be expressed as

$$\begin{pmatrix} \{x_a^{(1)}\} \\ \{x_b^{(1)}\} \\ \{\theta_b^{(1)}\} \end{pmatrix} = [H^{(1)}] \begin{pmatrix} \{f_a^{(1)}\} \\ \{f_b^{(1)}\} \\ \{m_b^{(1)}\} \end{pmatrix} \tag{1}$$

$$\begin{pmatrix} \{x_c^{(2)}\} \\ \{x_b^{(2)}\} \\ \{\theta_b^{(2)}\} \end{pmatrix} = [H^{(2)}] \begin{pmatrix} \{f_c^{(2)}\} \\ \{f_b^{(2)}\} \\ \{m_b^{(2)}\} \end{pmatrix} \tag{2}$$

and

$$[H^{(1)}] = \begin{pmatrix} [TT_{aa}^{(1)}] & [TT_{ab}^{(1)}] & [TR_{ab}^{(1)}] \\ [TT_{ba}^{(1)}] & [TT_{bb}^{(1)}] & [TR_{bb}^{(1)}] \\ [RT_{ba}^{(1)}] & [RT_{bb}^{(1)}] & [RR_{bb}^{(1)}] \end{pmatrix} \tag{3}$$

$$[H^{(2)}] = \begin{pmatrix} [TT_{cc}^{(2)}] & [TT_{cb}^{(2)}] & [TR_{cb}^{(2)}] \\ [TT_{bc}^{(2)}] & [TT_{bb}^{(2)}] & [TR_{bb}^{(2)}] \\ [RT_{bc}^{(2)}] & [RT_{bb}^{(2)}] & [RR_{bb}^{(2)}] \end{pmatrix} \tag{4}$$

where x, θ, f, and m are displacement, angular displacement, force, and moment, respectively. $[H^{(1)}]$ and $[H^{(2)}]$ are the frequency response matrices of substructures (1) and (2), respectively. The superscripts (1) and

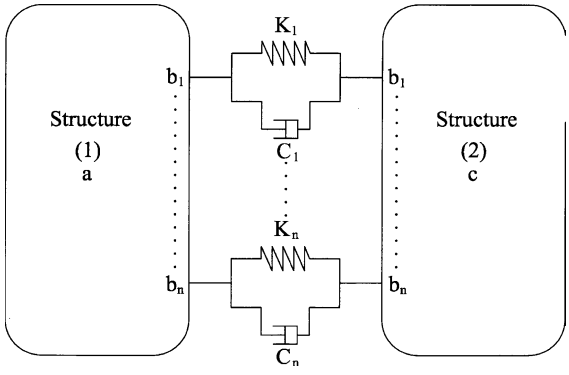

Fig. 1. Substructures and joints.

(2) refer to the substructures and the subscripts a, b, and c refer to the regions in the substructures.

The substructures are connected by joints and the equilibrium and compatibility conditions at the joints have to be fulfilled. Assuming no external force and moment acting on the joints, the conditions can be described as

$$\{f_b^{(1)}\} + \{f_b^{(2)}\} = 0 \tag{5}$$

$$\{m_b^{(1)}\} + \{m_b^{(2)}\} = 0 \tag{6}$$

$$\begin{Bmatrix} \{x_b^{(2)}\} - \{x_b^{(1)}\} \\ \{\theta_b^{(2)}\} - \{\theta_b^{(1)}\} \end{Bmatrix} = [H_J] \begin{Bmatrix} \{f_b^{(1)}\} \\ \{m_b^{(1)}\} \end{Bmatrix} \tag{7}$$

where $[H_J]$ is the frequency response matrix of the joints and is assumed to be

$$[H_J] = [P_J]^{-1} \tag{8}$$

$$[P_J] = [K_J] + j\omega[C_J] \tag{9}$$

We define the displacements and external forces for the integrated structure as

$$\{x^{(3)}\} = \begin{bmatrix} \{x_a^{(1)}\} \\ \{x_c^{(2)}\} \end{bmatrix} \tag{10}$$

$$\{f^{(3)}\} = \begin{bmatrix} \{f_a^{(1)}\} \\ \{f_c^{(2)}\} \end{bmatrix} \tag{11}$$

and the input–output relationship for the integrated structure is

$$\{x^{(3)}\} = [H^{(3)}]\{f^{(3)}\} \tag{12}$$

$$[H^{(3)}] = \left(\begin{bmatrix} [TT_{ab}^{(1)}] & [TR_{ab}^{(1)}] \\ -[TT_{cb}^{(2)}] & -[TR_{cb}^{(2)}] \end{bmatrix} [H_B]^{-1} \times \begin{bmatrix} -[TT_{ba}^{(1)}] & [TT_{bc}^{(2)}] \\ -[RT_{ba}^{(1)}] & [RT_{bc}^{(2)}] \end{bmatrix} + \begin{bmatrix} [TT_{aa}^{(1)}] & 0 \\ 0 & [TT_{cc}^{(2)}] \end{bmatrix} \right) \tag{13}$$

$$[H_B] = [H_J] + \begin{bmatrix} [TT_{bb}^{(1)}] + [TT_{bb}^{(2)}] & [TR_{bb}^{(1)}] + [TR_{bb}^{(2)}] \\ [RT_{bb}^{(1)}] + [RT_{bb}^{(2)}] & [RR_{bb}^{(1)}] + [RR_{bb}^{(2)}] \end{bmatrix} \tag{14}$$

where superscript (3) refers to the integrated structure, containing substructures (1) and (2), and the joints.

If the substructure (2) is assumed to be rigid and fixed, as shown in Fig. 2, $[H^{(2)}] = 0$ and Eq. (13) can be simplified as

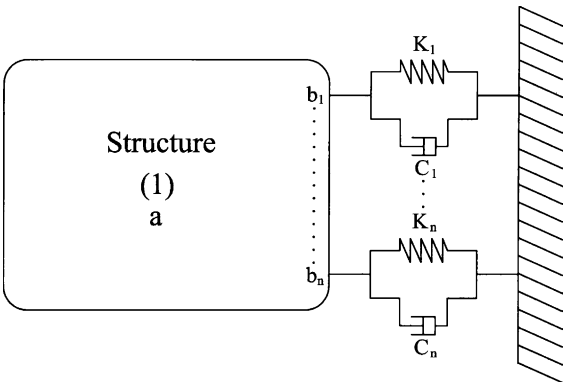

Fig. 2. Joints at the boundary of the structure.

$$[TT_{aa}^{(3)}] - [TT_{aa}^{(1)}] = \begin{bmatrix} [TT_{ab}^{(1)}] & [TR_{ab}^{(1)}] \end{bmatrix} [\overline{H}_B]^{-1} \begin{bmatrix} -[TT_{ba}^{(1)}] \\ -[RT_{ba}^{(1)}] \end{bmatrix} \tag{15}$$

where

$$[\overline{H}_B] = \begin{bmatrix} [TT_{bb}^{(1)}] & [TR_{bb}^{(1)}] \\ [RT_{bb}^{(1)}] & [RR_{bb}^{(1)}] \end{bmatrix} + [H_J] \tag{16}$$

Eqs. (15) and (16) are the equations for identification in this paper.

The difficulties of identification of joint parameters include the measurement of angular displacements and the exertion of moments, which are not easy [16]. Besides, the measurement at the joints may be obstructed by clamps or other joining mechanisms. The frequency response matrices of substructure (1) in Eqs. (15) and (16), including those related to the rotational degrees of freedom, $[TR_{ab}^{(1)}]$, $[RT_{ba}^{(1)}]$, $[RR_{bb}^{(1)}]$, can be obtained from experiment or finite element analysis for the unconstrained (or free–free) substructure (1). The frequency response matrix, $[TT_{aa}^{(3)}]$, relates only to the translational degrees of freedom in the non-joint region and can be obtained experimentally for the constrained structure, which includes substructure (1) and the joints.

If the number of measurement points in region a is m and the number of joints in region b is n, Eq. (15) becomes

$$[\Delta TT_{aa}]_{m\times m} = -\begin{bmatrix} [TT_{ab}^{(1)}] & [TR_{ab}^{(1)}] \end{bmatrix}_{m\times 2n} [Y]_{2n\times m} \tag{17}$$

where

$$[\Delta TT_{aa}]_{m\times m} = [TT_{aa}^{(3)}]_{m\times m} - [TT_{aa}^{(1)}]_{m\times m} \tag{18}$$

$$[Y]_{2n\times m} = [\bar{H}_B]_{2n\times 2n}^{-1} \begin{bmatrix} [TT_{ba}^{(1)}] \\ [RT_{ba}^{(1)}] \end{bmatrix}_{2n\times m} \tag{19}$$

Multiply both sides of Eq. (19) by $[\overline{H}_B]$, and substitute Eqs. (8) and (16) into Eq. (19). We obtain

$$[Y]_{2n\times m} = [P_J]_{2n\times 2n}\left(\begin{bmatrix}[TT_{ba}^{(1)}]\\ [RT_{ba}^{(1)}]\end{bmatrix} - \begin{bmatrix}[TT_{bb}^{(1)}] & [TR_{bb}^{(1)}]\\ [RT_{bb}^{(1)}] & [RR_{bb}^{(1)}]\end{bmatrix}[Y]\right)_{2n\times m} \quad (20)$$

where

$$[P_J]_{2n\times 2n} = [H_J]^{-1}_{2n\times 2n} = \left(\begin{bmatrix}[K_{tt}] & [K_{tr}]\\ [K_{rt}] & [K_{rr}]\end{bmatrix}_{2n\times 2n} + j\omega\begin{bmatrix}[C_{tt}] & [C_{tr}]\\ [C_{rt}] & [C_{rr}]\end{bmatrix}_{2n\times 2n}\right) \quad (21)$$

When $m \geqslant 2n$, Eqs. (17) and (20) can be solved by singular value decomposition (SVD) [17] for $[P_J]$ at each frequency. The noise effect can be reduced by more measurements in the non-joint regions, i.e., $m > 2n$. If the joint parameters, k_{ij} and c_{ij}, are considered as constants, the values of frequency response at multiple frequencies can be assembled to form an over-determined set of equations and solved by SVD to reduce the noise effect.

The structure under experiment in this paper consists of a beam with a joint at one end. Since $n = 1$, $m \geqslant 2$ is enough for the solving of the joints parameters in this case. Two models of the joint are considered, without damping presently,

$$\text{Model A: } \begin{bmatrix}K_{tt} & 0\\ 0 & K_{rr}\end{bmatrix} \quad (22)$$

$$\text{Model B: } \begin{bmatrix}K_{tt} & K_{tr}\\ K_{rt} & K_{rr}\end{bmatrix} \quad (23)$$

Model B contains the coupled terms of translational and rotational stiffness.

3. Results and discussion

The tested structure is shown in Fig. 3. Point J is the location of the joint, and points 1 and 2 are the measurement locations. Dimensions and material coefficients are listed in Table 1. The values of the material coefficients are obtained through a least square procedure using the natural frequencies of the beam under free–free condition. Two-dimensional beam element was used in the finite element modeling for the structure, as depicted in Fig. 3. The experimental and simulated results of FRF (receptance), TT_{22}, show good agreement in Fig. 4 and Table 2, which means we can use the finite element model to provide the necessary FRFs of the structure under unconstrained condition for identification.

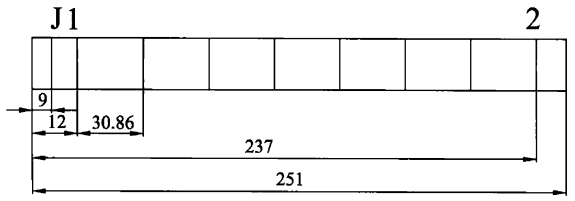

Fig. 3. Finite element model of the beam (with dimension in mm).

Table 1
Dimensions and material properties of the structure

Dimensions (m)	
h	0.00216
w	0.03492
L	0.251
Material properties	
Elastic modulus (GPa)	61.355
Density (kg/m^3)	2514.23
Poisson's ratio	0.33

The constrained structure is screwed on a table during the experiment, as shown in Fig. 5. The stainless steel screw is M6 with a length 18.8 mm. A torque of 9.81 N-m (100 kg-cm) is applied on the screw. Two nuts are put between the beam and the table. The height of the nuts is

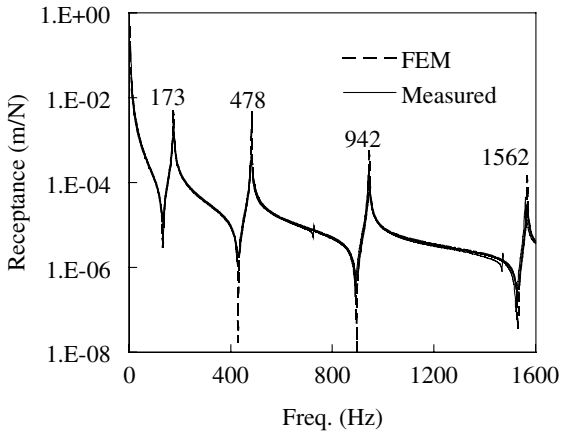

Fig. 4. FRF (TT_{22}) results of experiment and finite element analysis for the unconstrained beam.

Table 2
Comparison of natural frequency of unconstrained structure

Natural frequency (Hz)	FEM	Modal testing
1	174.08	173
2	479.94	478
3	941.85	942
4	1561.5	1562

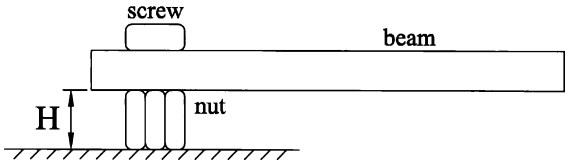

Fig. 5. Assembly of beam and screw.

$H = 8.64$ mm. An impulse hammer, Dytran 5802A, and an accelerometer, Endevco 2250 A-10, were used to excite the structure and measure the response respectively. The dynamic spectrum analyzer, HP35665A, was used to acquire the measurement data.

Although using more measurement points can reduce the noise effect and improve the accuracy of the results, only two measurement points, points 1 and 2 in Fig. 3, were used in the experiment to demonstrate the effectiveness of the method. Figs. 6 and 7 show the identified results of the joint parameters of model A, where large error peaks appear at 173, 190, 378, 518, 1018, 1044, and 1148 Hz. These frequencies are the natural frequencies of the beam under constrained and unconstrained conditions. The reason for the error peaks is the identification procedure utilizes the FRFs under both conditions and the FRFs at resonance are not accurate enough. The values of K_{tt} seem not constant during the bandwidths of 700–1000 Hz and 1300–1600 Hz, but the values of K_{rr} are more conformed to a constant in each given bandwidth.

We might assume the joint stiffness is constant in each given bandwidth and average the identified results within each bandwidth. The averaged stiffness values are listed in Table 3. Fig. 8 shows the simulation results of frequency response (receptance) using the averaged values, FEM_1 and FEM_2, of joint stiffness in bandwidth 1 and 2, respectively. The frequencies response

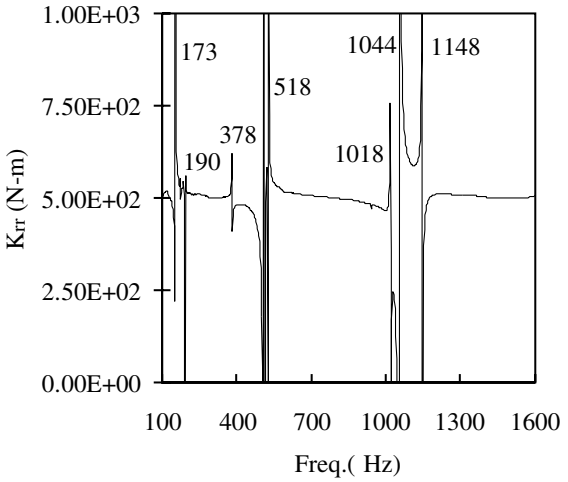

Fig. 7. Identified results of K_{rr}, model A.

Table 3
Averaged results of identified stiffness

	Band 1 (600–950 Hz)	Band 2 (1300–1600 Hz)
K_{tt} (N/m)	4.3158E6	4.4352E6
K_{rr} (N-m)	500.33	502.77

functions using FEM_1 and FEM_2 almost coincide in the frequency range. The simulation also shows the modes at 28, 190, 532, and 1044 Hz, which correspond to the modes of 32, 188, 520, and 1018 Hz from experiment. However, the modes of 378 and 1148 Hz from experiment do not show up in the simulation results. Furthermore, the simulated natural frequencies are higher than those from experiment except mode 1.

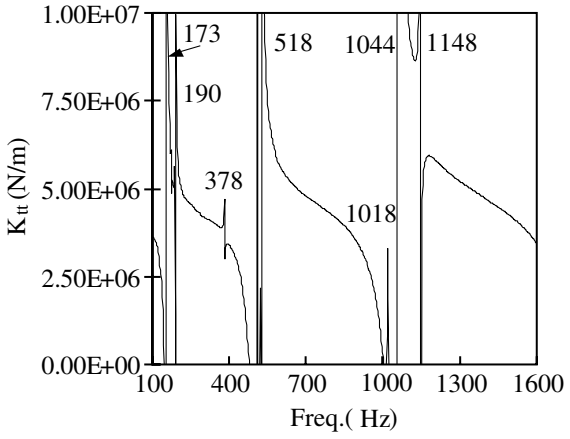

Fig. 6. Identified results of K_{tt}, model A.

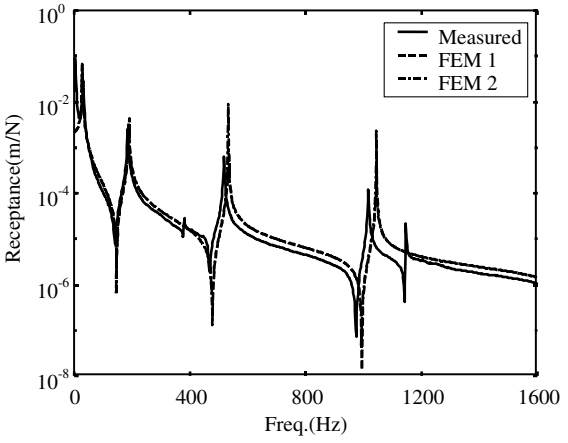

Fig. 8. FRF (TT_{22}) results of experiment and FEM for the constrained beam.

From a sensitivity analysis of the natural frequency to the joint stiffness [18], Figs. 9 and 10 are the changes of natural frequency of the first mode with joint stiffness, K_{tt} and K_{rr}, respectively. we found that the identified values of K_{tt} in Table 3 is located outside the sensitive zone (about 10–10^4 N/m, where the slope of natural frequency to K_{tt} is large), while the identified values of K_{rr} are located inside the sensitive zone (about 1–10^3 N-m). So even there is a difference of 1.194E5 N/m (=4.4352E6−4.3158E6) in translational stiffness of FEM_1 and FEM_2, their simulation results still agree well to each other. The identification inaccuracy of joint stiffness K_{tt} does not affect the FRFs too much in this case.

The reasons that cause the simulated natural frequencies to be higher than those from experiment, except mode 1 in Fig. 8, may be due to (1) insufficient element number in the finite element modeling, and (2) over-restriction on the joint model. The first reason was excluded by a convergence test by increasing the element number in the modeling of the structure. The second reason was studied by using joint model B, in which additional coupled terms are added.

Figs. 11–13 are the identification results of the joint parameters using model B, where large error peaks appear at 173, 190, 378, 518, 1018, 1044, and 1148 Hz. Again, these frequencies are the natural frequencies of the structure under constrained and unconstrained conditions, and due to the fact that the FRFs at resonance are not accurate enough.

The identified values of joint parameters at some specific frequencies are listed in Table 4. The identified

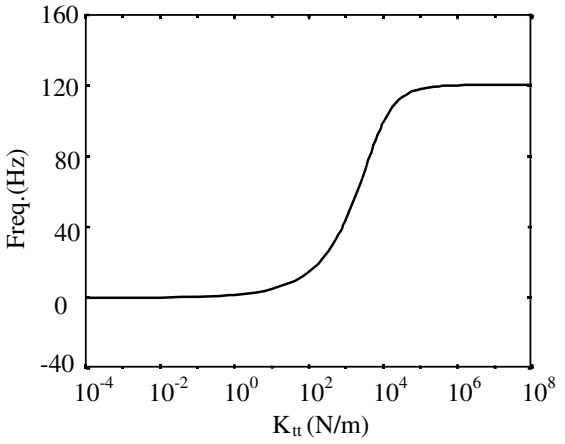

Fig. 9. Change of natural frequency of mode 1 with K_{tt} ($K_{rr}=0$).

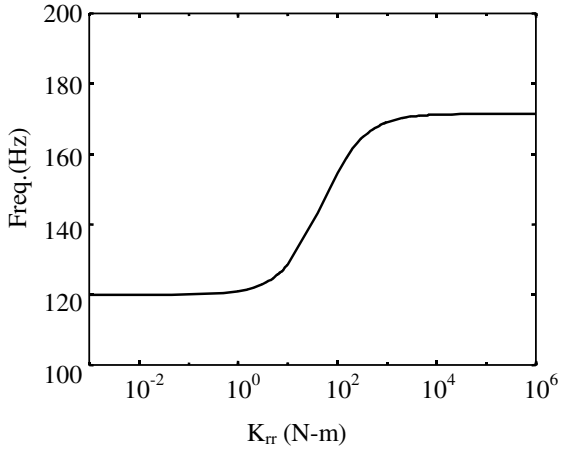

Fig. 10. Change of natural frequency of mode 1 with K_{rr} ($K_{tt}=\infty$).

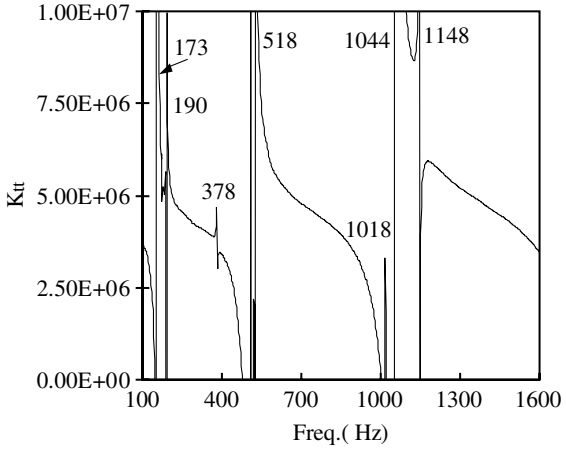

Fig. 11. Identified results of K_{tt}, model B.

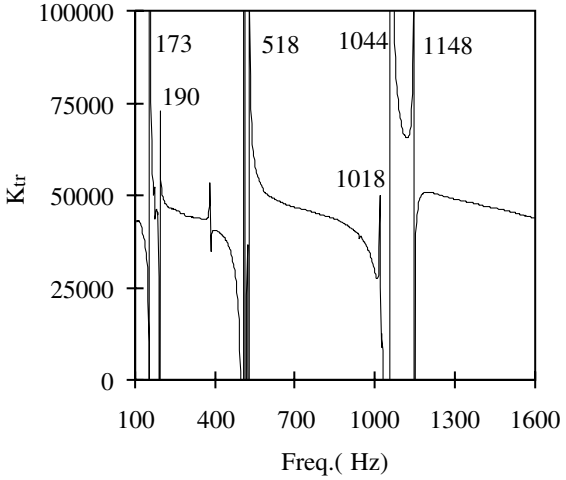

Fig. 12. Identified results of K_{tr}, model B.

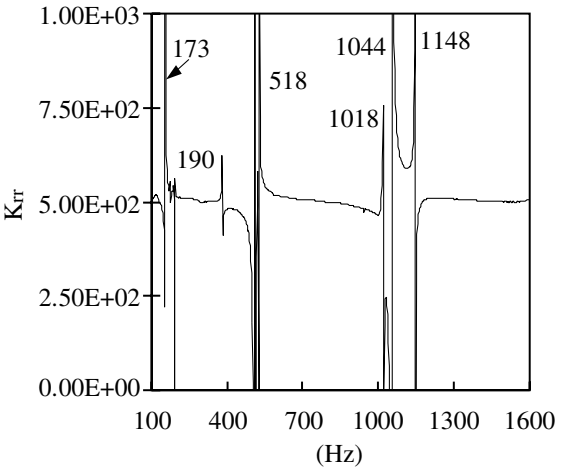

Fig. 13. Identified results of K_{rr}, model B.

Table 4
Identified results at specific frequencies

Hz	K matrix	
250	4.5468E6	4.6037E4
	4.6037E4	5.0952E2
700	4.7819E6	4.6721E4
	4.6721E4	5.0596E2
1500	4.2147E6	4.5730E4
	4.5730E4	5.0029E2

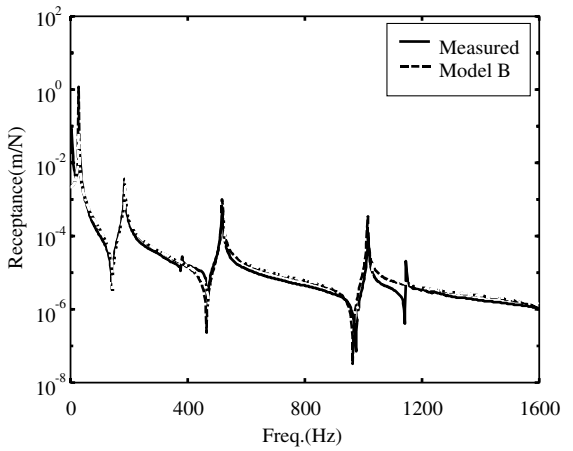

Fig. 14. FRF (TT_{22}) results of experiment and finite element analysis for the constrained beam, model B.

results are different at different frequencies, but the discrepancies of K_{rr} are the least.

Fig. 14 shows the comparison of experimental results and simulation results using the identified results of joint model B, where the agreement is much better than that in Fig. 8, especially for higher modes. The accuracy of the simulated natural frequencies is greatly improved by using joint model B.

The simulated results lack the modes of 378 and 1148 Hz in Figs. 8 and 14. This is because of using the two-dimensional beam element in the finite element modeling. The modes of 378 and 1148 Hz are torsional modes and cannot be modeled by the two-dimensional beam element, since torsional modes are three-dimensional. Hexahedron elements were used in the finite element modeling and 6 modes appeared in the frequency range of 0–1600 Hz, where the torsional modes (modes 3 and 6) are confirmed by the mode shapes [18].

4. Conclusions

This paper used the substructural synthesis method to derive the identification equations and to identify the joint parameters including the rotational stiffness. From the results of experiment and simulation, the following conclusions can be obtained:

(1) Finite element modeling is very accurate for unconstrained (or free–free) structures. The FRFs related to rotational degrees of freedom can be obtained by finite element modeling for the unconstrained structures, to overcome the experimental difficulties of angular displacement measurement and external moment exertion.
(2) The merit of the identification method is that the FRFs of the constrained structure relate only to the translational degrees of freedom in the non-joint region. All the measurements required for calibration and identification are made in the non-joint region and can be obtained easily by experiment.
(3) Identification results of joint parameters have large error peaks at the natural frequencies of the structure under constrained and unconstrained conditions, due to the fact that the FRFs at resonance are not accurate enough.
(4) The identification accuracy of joint parameters depends on the sensitivity of joint parameters. For the tested joint in this paper, the translational stiffness is not sensitive, while the rotational stiffness is sensitive. The identified results of the rotational stiffness are better conformed to a constant in each frequency zone. However, the identification inaccuracy of the translational stiffness does not affect the FRFs too much.
(5) Joint model B is studied, which is of matrix form and additional coupled terms are added in. The accuracy of the simulated natural frequencies is greatly improved by using joint model B.

(6) If torsional modes appear in the frequency range, two-dimensional elements are not capable of simulating the three-dimensional modes properly. Three-dimensional elements, such as 3D beam elements or hexahedron elements, are necessary in the finite element modeling.

Damping parameters of the joint have not been investigated in this paper, which will be the topics for future study.

References

[1] Beards CF. The damping of structural vibration by controlled interfacial slip in joints. ASME Publ, 81-DET-86, 1986.
[2] Ren Y, Beards CF. On the importance of weighting for FRF joint identification. In: The 11th International Modal Analysis Conference, Florida, USA, 1993.
[3] Nobari AS, Robb DA, Ewins DJ. Model updating and joint identification methods: applications, restrictions an overlap. Modal Anal: Int J Anal Exp Modal Anal 1993; 8(2):93–105.
[4] Inamura T, Sata T. Stiffness and damping properties of the elements of a machine tool structure. Ann CIRP 1979;28: 235–9.
[5] Yuan JX, Wu SM. Identification of the joint structural parameters of machine tool by DDS and FEM. ASME Trans J Eng Ind 1985;107:64–9.
[6] Yang KT, Park YS. Joint structural parameter identification using a subset of frequency response function measurements. Mech Syst Signal Process 1993;7: 509–30.
[7] Tsai JS, Chou YF. The identification of dynamics characteristics of a single bolt joint. J Sound Vib 1988;125(3): 487–502.
[8] Wang JH, Liou CM. Experimental identification of mechanical joint parameters. J Vib Acoust 1991;113:28–36.
[9] Hong SW, Lee CW. Identification of linearised joint structural parameter by combined use of measured and computed frequency responses. Mech Syst Signal Process 1991;5:267–77.
[10] Hwang HY. Identification techniques of structure connection parameters using frequency response function. J Sound Vib 1998;212(3):469–79.
[11] Ren Y, Beards CF. On substructure synthesis with FRF data. J Sound Vib 1995;185(5):845–66.
[12] Yang MJ. The development of the method of the dynamic parameters identification of the mechanical joints. Master Thesis, Department of Mechanical Engineering, National Tsing Hua University, Taiwan (in Chinese), 1996.
[13] Barker DB, Chen YS. Modeling the vibration restraints of wedge lock card guides. ASME Trans J Electron Packag 1993;115:189–94.
[14] Baruh H, Boka JB. Modeling and identification of boundary conditions in flexible structures. Int J Anal Exp Modal Anal 1993;8:107–17.
[15] Lin CH, Yang T, Chen YS, Fan SH, Tseng WH. Dynamic analysis of wedge-lock retainers for PC boards. In: The 16th National Conference of Mechanical Engineering, Taiwan (in Chinese), 1999. p. 225–31.
[16] Ewins DJ. Modal testing: theory and practice. England: Research Studies Press Ltd.; 1986.
[17] Leon SJ. Linear algebra with applications. 4th ed. Englewood Cliffs, New Jersey: Prentice Hall Inc.; 1994.
[18] Fan SH. A practical study on the identification of joint parameters. Master Thesis, Department of Mechanical Engineering, Yuan Ze University, Taiwan (in Chinese), 2002.